The Yang–Lee zeros of the 1D Blume–Capel model on connected and non-connected rings

2005 J. Phys. A: Math. Gen. 38 6863

(http://iopscience.iop.org/0305-4470/38/31/001)

INSTITUTE OF PHYSICS PUBLISHING JOURNAL OF PHYSICS A: MATHEMATICAL AND GENERAL

J. Phys. A: Math. Gen. **38** (2005) 6863–6877 doi:10.1088/0305-4470/38/31/001

The Yang–Lee zeros of the 1D Blume–Capel model on connected and non-connected rings

Luis A F Almeida and D Dalmazi

UNESP—Campus de Guaratinguetá-DFQ, Av. Dr. Ariberto P. da Cunha, 333, CEP 12516-410 Guaratinguetá, SP, Brazil

E-mail: luisaug@feg.unesp.br and dalmazi@feg.unesp.br

Received 24 May 2005, in final form 21 June 2005
Published 20 July 2005
Online at stacks.iop.org/JPhysA/38/6863

Abstract

We carry out a numerical and analytic analysis of the Yang–Lee zeros of the 1D Blume–Capel model with periodic boundary conditions and its generalization on Feynman diagrams for which we include sums over all connected and non-connected rings for a given number of spins. In both cases, for a specific range of the parameters, the zeros originally on the unit circle are shown to depart from it as we increase the temperature beyond some limit. The curve of zeros can bifurcate and become two disjoint arcs as in the 2D case. We also show that in the thermodynamic limit the zeros of both Blume–Capel models on the static (connected ring) and on the dynamical (Feynman diagrams) lattice tend to overlap. In the special case of the 1D Ising model on Feynman diagrams we can prove for arbitrary number of spins that the Yang–Lee zeros must be on the unit circle. The proof is based on a property of the zeros of Legendre polynomials.

PACS numbers: 05.50.+q, 05.70.Fh, 64.60.Cn, 75.10.Hk

1. Introduction

More than 50 years ago C N Yang and T D Lee initiated a theory [1] for studying phase transitions based on the partition function zeros. The same authors proved the celebrated circle theorem in [2]. It ensures, in particular, that the zeros of the $s = 1/2$ Ising model partition function on a given lattice occur only at pure imaginary values of the magnetic field. Defining $u = e^{-2\beta H}$ this implies that the zeros are on the unit circle in the complex u plane. The theorem is very robust and does not depend on details of the lattice such as space dimensionality, number of nearest neighbours or topology. Later, the circle theorem was generalized to higher spin models without [3] and with [4] extra symmetric potentials,

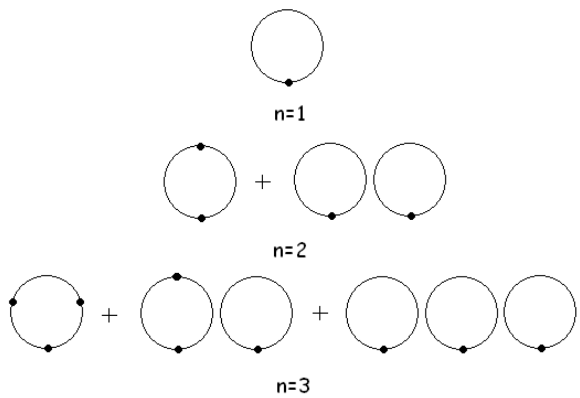

Figure 1. The Feynman diagrams corresponding to $\mathcal{Z}_1^{nc}$, $\mathcal{Z}_2^{nc}$ and $\mathcal{Z}_3^{nc}$.

as well as to ferroeletric models [5] and some Heisenberg models [5–7]. In all these models the spin variables are defined on a given static lattice and therefore they are the only relevant degrees of freedom. The proofs are based on the fact that the partition functions can be written as polynomials of a specific form [2]. Since addition of polynomials mix up their zeros in a rather non-trivial way, it is unexpected that the circle theorem will hold for spin models defined on dynamical random lattices which are themselves also degrees of freedom and must be summed over altogether with the spins. However, numerical results for the Ising model defined on 2D dynamical random lattices of planar [8–10] and torus topology [11] indicate that the Yang–Lee zeros do lie on the unit circle although no circle theorem is known in the case of dynamical lattices. It is not even clear whether the new polynomials are of the form assumed in [2]. In particular, the form of the polynomials used in [2] is not kept by arbitrary linear combinations. The dynamical lattices used in [8–11] were suggested in [12] in order to mimic the effects of 2D fluctuating random surfaces in the continuum limit (2D gravity). The partition functions were generated by $N \times N$ Hermitian random matrices and the 2D gravity interpretation is achieved by fine tuning the coupling constants in the model and taking $N \to \infty$ simultaneously. For the special case where the matrices become numbers ($N = 1$) [13], although the 2D gravity interpretation is lost, the models defined on the so-called thin graphs exhibit phase transitions with mean field exponents and strong similarities with models defined on the Bethe lattice [14]. In this case the partition function is obtained by summing over spin variables and connected and non-connected regular graphs (non-connected Feynman diagrams). Once again, numerical results valid for finite number of spins [11] and analytic results valid in the thermodynamic limit [15, 16] strongly support a circle theorem for this type of random lattice but no explicit proof for finite number of spins has ever been given. It is the purpose of this work to produce such a proof at least in the simplified case of one-dimensional models where the random graphs become connected and non-connected rings (see figure 1). We have chosen the ferromagnetic Blume–Capel (BC) model [17] since it is the simplest model with 'would be' $\mathcal{Z}_2$ symmetry such that on one hand their zeros, in any dimension, are known to satisfy the circle theorem in a certain parameters range [4] and on the other hand they have been shown in 2D to exhibit non-trivial topological properties like bifurcation for other range of the parameters [18]. Besides, the BC model includes the $s = 1/2$ and $s = 1$ Ising models.

2. The 1D Blume–Capel model on non-connected rings

In the spin one Ising model there are three spin states on each site: $S_i = -1, 0, 1$. The Blume–Capel (BC) model is a generalization of the spin one Ising model where, besides the magnetic field H which works as a source for dipole interaction, we now introduce a coupling λ functioning as a source for quadrupole interactions such that we still have a 'would be' $\mathcal{Z}_2$ symmetry by exchanging $H \to -H$. The energy and the partition function of the Blume–Capel model are given by

$$E = -J\sum_{\langle ij\rangle} S_i S_j - H\sum_{i=1}^{n} S_i - \lambda\sum_{i=1}^{n}\left(1 - S_i^2\right) \tag{1}$$

$$Z_n = \sum_{\{S_i\}} \exp\left(K\sum_{\langle ij\rangle} S_i S_j + \sum_{i=1}^{n}\left[hS_i + \Delta\left(1 - S_i^2\right)\right]\right). \tag{2}$$

We only work with the ferromagnetic case $J > 0$. The sum $\sum_{\langle ij\rangle}$ is over nearest-neighbour sites. For the one-dimensional model we assume periodic boundary conditions $S_j = S_{n+j}$. In this case the lattice becomes a ring with n sites (vertices) and n bonds. Throughout this work we use the following definitions:

$$\begin{aligned} K &= J/kT; \qquad & c &= \mathrm{e}^{-K} \\ h &= H/kT; \qquad & u &= \mathrm{e}^{h} \\ \Delta &= \lambda/kT; \qquad & x &= \mathrm{e}^{\Delta}. \end{aligned} \tag{3}$$

Although originally suggested in a magnetic context [17], the BC model corresponds to a special case of the BEG model [19] and it can be used to describe phase separation driven by superfluidity in $\mathrm{He}^{(3)}$–$\mathrm{He}^{(4)}$ mixtures. Its phase diagram in 2D is rich, including tricriticallity. At $x = 0(\Delta \to -\infty)$ it becomes the $s = 1/2$ Ising model while for $x = 1(\Delta = 0)$ it corresponds to the $s = 1$ Ising model.

Each configuration with p spins down, n_0 spins zero and n_{ab} bonds connecting spins a to b, where $a, b = +, -, 0$ correspond to spins up, down and zero respectively, will contribute to the partition function a factor:

$$\exp([(n - p - n_0)h - ph + n_0\Delta])\exp([K(n_{++} + n_{--}) - Kn_{+-}]). \tag{4}$$

That factor will be needed in order to define the model on Feynman diagrams below. We start with the following generating function of Feynman diagrams in a zero-dimensional field theory:

$$\begin{aligned} G(h, c, \Delta, g) &= \frac{\int \mathrm{d}\phi_+\,\mathrm{d}\phi_-\,\mathrm{d}\phi_0 \exp\left(-\frac{1}{2}\left[\phi_a M_{ab}\phi_b - g\left(\mathrm{e}^{h}\phi_+^2 + \mathrm{e}^{-h}\phi_-^2 + \mathrm{e}^{\Delta}\phi_0^2\right)\right]\right)}{\int \mathrm{d}\phi_+\,\mathrm{d}\phi_-\,\mathrm{d}\phi_0\, \mathrm{e}^{-\frac{1}{2}[\phi_a M_{ab}\phi_b]}} \\ &\equiv \left\langle \exp\left(\frac{g}{2}\left(\mathrm{e}^{h}\phi_+^2 + \mathrm{e}^{-h}\phi_-^2 + \mathrm{e}^{\Delta}\phi_0^2\right)\right)\right\rangle \end{aligned} \tag{5}$$

where the coupling constant g will play the role of a counting parameter while the 3×3 symmetric matrix $M_{ab}, a, b = +, -, 0$ is to be determined from the Boltzmann weights in (2) for $h = 0 = \Delta$. The zero-dimensional fields $\phi_\pm, \phi_0$ will represent the spin states $S_i = \pm 1, 0$ respectively.

The expansion:

$$G(h, c, g) = \sum_{n=0}^{\infty} g^n \mathcal{Z}_n^{nc}, \tag{6}$$

defines the coefficients

$$\mathcal{Z}_n^{nc} = \frac{1}{2^n n!}\big\langle \big(\mathrm{e}^h\phi_+^2 + \mathrm{e}^{-h}\phi_-^2 + \mathrm{e}^{\Delta}\phi_0^2\big)^n\big\rangle. \tag{7}$$

If we interpret $\mathrm{e}^h\phi_+^2$, $\mathrm{e}^{-h}\phi_-^2$ and $\mathrm{e}^{\Delta}\phi_0^2$ as interaction vertices representing sites with up, down and vanishing spins respectively, the $\mathcal{Z}_n^{nc}$ have an interpretation as a diagrammatic expansion *a la* Feynman. In figure 1 we draw them for $n = 1, 2, 3$. The $\mathcal{Z}_n^{nc}$ correspond to the sum of all diagrams with a total of n interaction vertices such that each vertex has two lines attached and all lines must be connected as in figure 1. Each vertex must be of course of type up, down or zero and will carry a factor e^h, e^{-h} and e^{Δ}, respectively. Thus, we end up summing over all spin configurations altogether with all connected and non-connected rings with n vertices. The superscript 'nc' stands for non-connected since the expansion includes non-connected diagrams like the second one in the second row and the second and third ones in the third row of figure 1. Each internal line of the diagram connecting a vertex of type a to a vertex of type b corresponds mathematically to a Gaussian integral $\langle\phi_a\phi_b\rangle = M_{ab}^{-1}$ see (5). Therefore, according to the so-called Feynman rules[1], each diagram with p minus and n_0 vanishing spin contains a factor

$$\exp([(n-p-n_0)h - ph + n_0\Delta])\prod_{a<b}\langle\phi_a\phi_b\rangle^{n_{ab}}. \tag{8}$$

In order to make more contact with the statistical model and match the above factor with (4) we require $\langle\phi_a\phi_b\rangle$ to be proportional to the Boltzmann weights in (2) calculated at $h = 0 = \Delta$. That is,

$$\langle\phi_a\phi_b\rangle = \mathbf{M}_{ab}^{-1} = \kappa\exp\left(-\frac{E_{ab}(h=0=\Delta)}{kT}\right) = \kappa\begin{pmatrix}\mathrm{e}^K & \mathrm{e}^{-K} & 1\\ \mathrm{e}^{-K} & \mathrm{e}^K & 1\\ 1 & 1 & 1\end{pmatrix}.$$

If we choose the overall constant $\kappa = c/[(1-c^2)(1-c)]$ we obtain a simple form for M_{ab} such that the generating function (5) becomes

$$G(c,h,\Delta,g) = \frac{\int \mathrm{d}\phi_+\,\mathrm{d}\phi_-\,\mathrm{d}\phi_0\,\mathrm{e}^{-S_g}}{\int \mathrm{d}\phi_+\,\mathrm{d}\phi_-\,\mathrm{d}\phi_0\,\mathrm{e}^{-S_{g=0}}} \tag{9}$$

with

$$S_g = \frac{1}{2}\big[\phi_+^2 + \phi_-^2 + f\phi_0^2 + 2c\phi_+\phi_- 2(1+c)(\phi_+ + \phi_-)\phi_0\big] - \frac{g}{2}\big(\mathrm{e}^h\phi_+^2 + \mathrm{e}^{-h}\phi_-^2 + \mathrm{e}^{\Delta}\phi_0^2\big) \tag{10}$$

and

$$f = \frac{(1+c)(1+c^2)}{c}. \tag{11}$$

The Gaussian integrals in (9) can easily be calculated implying

$$G(c,h,\Delta,g) = \left[\frac{(1-c^2)^2(1-c)}{P_3(g)}\right]^{1/2} \tag{12}$$

where

$$P_3(g) = (1-c^2)^2(1-c) - g(1-c^2)(\tilde{x}+A) + g^2[(1+c)(1+c^2) + A\tilde{x}] - g^3\tilde{x} \tag{13}$$

$$A = \mathrm{e}^h + \mathrm{e}^{-h}; \qquad \tilde{x} = xc = \mathrm{e}^{\Delta-K}. \tag{14}$$

[1] For a demonstration of the Feynman rules in a simple case see [20].

Therefore, from (6) we can write down $\mathcal{Z}_n^{nc}$ as

$$\mathcal{Z}_n^{nc} = \left\{\left[\frac{(1-c^2)^2(1-c)}{P_3(g)}\right]^{1/2}\right\}_{g^n} \tag{15}$$

or equivalently from (7)

$$\mathcal{Z}_n^{nc} = \frac{\int \mathrm{d}\phi_+\,\mathrm{d}\phi_-\,\mathrm{d}\phi_0\,\mathrm{e}^{-S_g}\left(\mathrm{e}^h\phi_+^2 + \mathrm{e}^{-h}\phi_-^2 + \mathrm{e}^{\Delta}\phi_0^2\right)^n}{2^n n!\int \mathrm{d}\phi_+\,\mathrm{d}\phi_-\,\mathrm{d}\phi_0\,\mathrm{e}^{-S_{g=0}}}. \tag{16}$$

It is instructive to relate $\mathcal{Z}_n^{nc}$ given in (15) or (16) with the usual partition functions of the one-dimensional BC model on a ring $\mathcal{Z}_n$ given in (2). The Feynman rules and our definition for the overall constant κ allow us to write the diagrammatic expansion:

$$\mathcal{Z}_n^{nc} = \left[\frac{c}{(1-c^2)(1-c)}\right]^n \sum_{\text{diagrams}} \frac{\mathcal{Z}_n(\text{diagram})}{S_n(\text{diagram})} \tag{17}$$

where the sum is over all diagrams with n vertices, connected and non-connected. The factor S_n is a positive real number called symmetry factor of the graph and it comes from the sum over all possible ways of connecting the vertices among each other to build the corresponding graph. The number of such possibilities we call A_n. According to our notation, see (7), and the Feynman rules $S_n = (2^n n!)/A_n$. In order to obtain A_n it is convenient to label the two lines of the ith vertex as (a_i, b_i). For example, for the case of connected rings, like the first diagrams on each row of figure 1, there will be a total of $2n$ labels, if we start with the label a_1 it can be linked with any of the labels a_j or b_j such that $j \neq 1$. Thus, we have $2n-2$ possibilities for the first connection. The yet non-connected label b_1 can be linked with the labels of any vertex but the first and the jth ones. Thus, there are $2(n-2)$ possibilities. If we keep going until no label is left unconnected we end up with $A_n = (2n-2)!!$ and $S_n(\text{connected ring}) = \frac{2^n n!}{(2n-2)!!} = 2n$. The symmetry factor of the non-connected diagrams can be similarly obtained. As an example, for $n=3$ (third row in figure 1) expansion (17) becomes

$$\mathcal{Z}_3^{nc} = \left[\frac{c}{(1-c^2)(1-c)}\right]^3 \left[\frac{\mathcal{Z}_3}{6} + \frac{\mathcal{Z}_1\mathcal{Z}_2}{8} + \frac{\mathcal{Z}_1^3}{48}\right]. \tag{18}$$

The general expansion for arbitrary n can be obtained as follows. First, it is well known in field theory that the connected diagrams can be singled out by taking the logarithm of the generating function. Using that $S_n = 2n$ for connected diagrams we have

$$\ln G(h, c, \Delta, g) = \sum_{n=1}^{\infty} \frac{1}{2n}\left[\frac{gc}{(1-c^2)(1-c)}\right]^n \mathcal{Z}_n, \tag{19}$$

where on the right-hand side we have only partition functions of connected rings. Exponentiating (19) and comparing with expansion (6) we have the generalization of (18) for an arbitrary number of vertices:

$$\mathcal{Z}_n^{nc}(c,h) = \left[\frac{c}{(1-c^2)(1-c)}\right]^n \left[\exp\left(\frac{g\mathcal{Z}_1}{2} + \frac{g^2\mathcal{Z}_2}{4} + \cdots + \frac{g^n\mathcal{Z}_n}{2n}\right)\right]_{g^n} \tag{20}$$

$$= \left[\frac{c}{(1-c^2)(1-c)}\right]^n \left[\frac{\mathcal{Z}_1^n}{2^n n!} + \cdots + \frac{\mathcal{Z}_1\mathcal{Z}_{n-1}}{4(n-1)} + \frac{\mathcal{Z}_n}{2n}\right]. \tag{21}$$

In particular, compared with (17), the symmetry factors of the non-connected diagrams are produced automatically. Expression (21) shows that a generalization of the circle theorem valid for $\mathcal{Z}_n$ to sums like $\mathcal{Z}_n^{nc}$ is non-trivial.

3. Yang–Lee zeros

3.1. 1D BC model on a connected ring

Before we start with the 1D BC model defined on Feynman diagrams we first study the zeros of the static lattice (one ring) model.

The partition function (2) is a polynomial on each of the variables c, x and u. In particular, $\mathcal{Z}_n$ is a polynomial of degree $2n$ in the 'fugacity' u. Concerning the Yang–Lee zeros on the complex u-plane, it was proven in [4] that they must satisfy the circle theorem for $0 \leqslant x \leqslant 2$ independently of lattice details such as topology, coordination number or space dimensionality. The proof, reproduced below, is based on the decomposition [3] of a spin one particle in a cluster of two spin one-half ones: $S_i = (\sigma_{i1} + \sigma_{i2})/2$, where $\sigma_{i1}; \sigma_{i2} = \pm 1$. After such decomposition we can rewrite, up to an overall constant, $\mathcal{Z}_n$ as a partition function of a bigger system with $2n$ spin one-half particles:

$$\mathcal{Z}_n \propto \tilde{\mathcal{Z}}_{2n} = \sum_{\{\sigma_\alpha\}} \exp\left[\sum_{\langle\alpha\beta\rangle} \tilde{K}_{\alpha\beta}\sigma_\alpha\sigma_\beta + \frac{h}{2}\sum_{\alpha=1}^{2n}\sigma_\alpha\right] \tag{22}$$

where σ_α include all σ_{i1} and σ_{i2} with $i = 1, \ldots, n$. The sum $\sum_{\langle\alpha\beta\rangle}$ runs over all nearest neighbours (n.n.), including spins in the same cluster. The new coupling is

$$\tilde{K}_{\alpha\beta} = \begin{cases} \frac{1}{2}(\ln 2 - \Delta) & \text{within a cluster.} \\ K/4 & \text{between n.n. of different clusters.} \end{cases} \tag{23}$$

The factor $\ln 2/2$ comes from the double degeneracy of the $S = 0$ state which can be represented inside a cluster by the weight $W(\sigma_\alpha, \sigma_\beta) = \exp\left[\frac{1}{2}\ln 2(\sigma_\alpha\sigma_\beta - 1)\right]$. Since the circle theorem holds for any ferromagnetic partition function of the form (22) we conclude that for $\Delta \leqslant \ln 2\,(0 \leqslant x \leqslant 2)$, see [4], the Yang–Lee zeros of the BC model will lie on the unit circle for any space dimension.

To the best of our knowledge, even though we will be dealing with the exactly solvable one-dimensional model, there are no exact analytic results about the Yang–Lee zeros of the BC model for $\Delta > \ln 2$. The best we can do is to present what we found numerically for finite number of spins and deduce approximate analytic results along the lines of the work of [21] for the one-dimensional Potts model. The starting point for the numerical calculations of the zeros is the exact expression for $\mathcal{Z}_n$ which can be obtained, for instance, by inverting expansion (19) using (12),

$$\mathcal{Z}_n = 2n\left[\frac{(1-c^2)(1-c)}{c}\right]^n \left\{\ln\left[\frac{(1-c^2)^2(1-c)}{P_3(g)}\right]^{1/2}\right\}_{g^n} \tag{24}$$

$$= \left(\lambda_+^n + \lambda_-^n + \lambda_0^n\right)/c^n \tag{25}$$

where $\lambda_\pm$ and λ_0 are solutions of the cubic equation:

$$\lambda^3 - \lambda^2(A + \tilde{x}) + \lambda[A(1-c)\tilde{x} + 1 - c^4] - \tilde{x}(1-c^2)(1-c)^2 = 0. \tag{26}$$

Incidentally, we note that the inversion of formula (19) is a diagrammatic method alternative to the transfer matrix approach. The quantities $\lambda_\pm/c$; λ_0/c are precisely the eigenvalues of the transfer matrix of the 1D BC model, although we never really used it in our derivation of (25) which came from factorizing $P_3(g)$. We remark that the way we found the exact solution (25) is a combinatorial one, where the Feynman rules take care of the correct combinatorial factors. In this sense it is similar to the original solution of the one-dimensional Ising model by Ising [23].

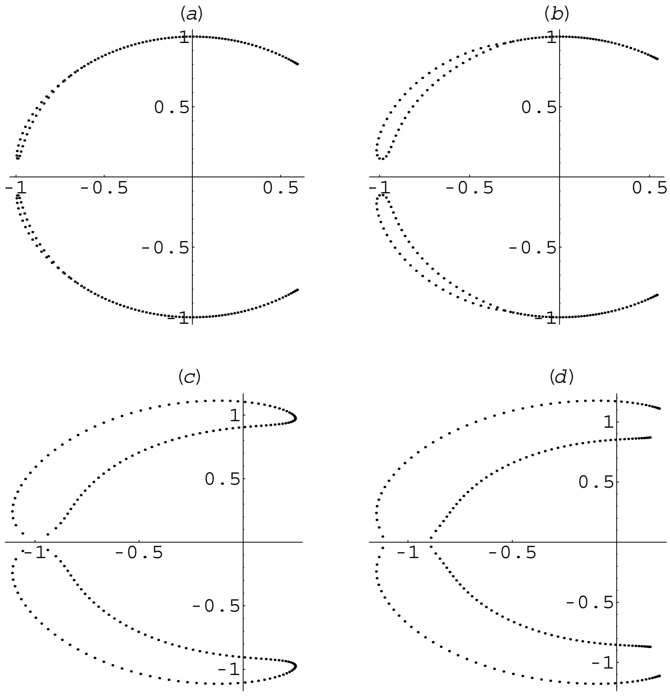

Figure 2. Yang–Lee zeros of the usual 1D Blume–Capel model on the complex e^h plane for $x = 3$ and temperatures $c = 0.435, 0.450, 0.500$ and 0.520 respectively, in 2(*a*)–(*d*).

Proceeding further, for the purpose of generating the exact partition functions for large n it turned out to be faster to use expression (24) instead of plugging, for fixed c and $\tilde{x}$, the solution of (26) in (25). For other higher spin models $s > 1$ the computational advantage of (24) against (25) is even bigger. Given the exact expressions for the partition function, we have numerically obtained their zeros using the software Mathematica. Among other checks we have used the exact analytic results for the zeros of the 1D Ising model on one ring to confirm the accuracy of the zeros. As a general feature we have found numerically that the complex $u = e^h$ zeros never converge for non-zero temperatures to the positive real axis in agreement with the fact that no phase transition for real magnetic fields appears in one-dimensional spin models with short range interaction. Furthermore, the zeros lie on the unit circle for $0 \leqslant x \leqslant 2$ and arbitrary temperatures $0 \leqslant c \leqslant 1$, thus confirming the analytic result of [4]. For any given $x > 2$ we have always been able to find a temperature after which the zeros departure from the unit circle as shown in figures 2(*a*)–(*d*).

As x increases the minimal temperature for which that happens decreases. As a general rule, increasing x or c or even both of them the zeros move in such a way that after a given value for the product $xc = e^{\Delta - K}$ they start bifurcating into two branches: one inside and the other outside the unit circle. A bifurcation of the Yang–Lee zeros has been also observed in the two-dimensional BC model [18] but in that case the bifurcation starts at $\theta = 0$ instead of $\theta = \pi$. Our numerical results show that in the interval $0 \leqslant \tilde{x} \leqslant 1$ the zeros lie on the unit circle.[2] Although we have not been able to deduce a rigorous proof of this fact analytically,

[2] The numerical results presented in [18] at a fixed temperature in the 2D case are in approximate agreement with the interval $0 \leqslant \tilde{x} \leqslant 1$, where $e^{-\lambda}$ of that reference corresponds to $\tilde{x} = cx$; see the comment below figure 1 of that reference.

we have approximate analytic results based on the approach of [21]. The main idea is that the zeros of (25) appear whenever at least two transfer matrix eigenvalues have the same absolute value which on its turn must be bigger than the absolute value of the remaining eigenvalue, e.g., $|\lambda_+| = |\lambda_-| > |\lambda_0|$. Unfortunately, differently from the Q-state Potts model treated in [21] which is similar to the Ising model ($Q = 2$), the secular equation (26) is not easily factorizable and their explicit solutions are not very useful to match absolute values. We have to stick to approximate solutions. In order to keep some similarity to the Ising model ($x = 0$), we solve (26) as a series expansion for low $\tilde{x}$. That gives

$$\lambda_0 = \frac{(1-c^2)^2\tilde{x}}{(1+c^2)} - \frac{2Ac(1-c)^2\tilde{x}^2}{(1+c^2)^3} + \mathcal{O}(\tilde{x}^3) \tag{27}$$

$$\lambda_\pm = \sqrt{1-c^4}\, g_\pm + [c + \frac{2c^3}{(1+c^2)\big(g_\pm^2 - 1\big)}]\tilde{x} + \mathcal{O}(\tilde{x}^2) \tag{28}$$

where

$$g_\pm = \frac{A}{\sqrt{1-c^4}} \pm \left[\left(\frac{A}{\sqrt{1-c^4}}\right)^2 - 1\right]^{1/2}. \tag{29}$$

The singularity at $g_\pm^2 = 1$ is the Yang–Lee edge singularity ($\lambda_+ = \lambda_-$) of the Ising model ($\tilde{x} = 0$). Since $g_+g_- = 1$ we can write $g_+ = \rho\,\mathrm{e}^{\mathrm{i}\theta}$ and $g_- = \mathrm{e}^{-\mathrm{i}\theta}/\rho$. Therefore, we write $|\lambda_+|^2 = r(\rho,\theta,c,\tilde{x})r(\rho,-\theta,c,\tilde{x})$ and $|\lambda_-|^2 = r(1/\rho,-\theta,c,\tilde{x})r(1/\rho,\theta,c,\tilde{x})$ for some function $r(a,b,c,d)$. Thus, assuming $\rho = 1(A = \cosh(h) = \sqrt{1-c^4})$, which leads us to the unit circle $|\mathrm{e}^h| = 1$ since $0 \leqslant \cosh(h) \leqslant 1$, we have $|\lambda_+| = |\lambda_-|$. Therefore, our assumption will lead in fact to zeros on the unit circle if $\delta_\pm = |\lambda_\pm| - |\lambda_0| > 0$, or equivalently $\delta_\pm = \Re e(f_\pm - f_0) > 0$ where $f_i = \ln\lambda_i$. This can be checked from (27) and (28). Using our assumption $g_\pm = \mathrm{e}^{\pm \mathrm{e}\theta}$ we get

$$\delta_\pm = \frac{1}{2}\ln\left[\frac{(1+c^2)^3(1+c)}{(1-c)^3}\right] - \ln\tilde{x} + \tilde{x}c\left[\frac{5\cos\alpha}{(1+c^2)^2}\right] + \mathcal{O}(\tilde{x}^2) \tag{30}$$

where $h \equiv \mathrm{i}\alpha$, consequently $\cos\theta = \cos\alpha/\sqrt{1-c^4}$. The first term on the right-hand side of (30) is always positive and the second one shows why the zeros go to the unit circle for $0 \leqslant \tilde{x} \leqslant 1$. The third term is also in agreement with our numerical calculations since it is more negative, thus pushing the zeros outside the unit circle, for angles close to $\alpha = \pi$. Adding up the three terms we have checked that $\delta_\pm > 0$ whenever $\tilde{x} \leqslant \tilde{x}^*$ where the minimum value for $\tilde{x}^*_{\min} = 0.780(2)$ occurs at $c = 0.220(5)$ and $\alpha = \pi$. The fact that $\tilde{x}^*_{\min} \neq 1$ is an artefact of the low $\tilde{x}$ approximation. In practice our numerical calculation of the zeros shows that they lie on the unit circle for $0 \leqslant \tilde{x} \leqslant 1$ with great accuracy. Although that seems to be a weak form (temperature dependent) of the circle theorem, one can slightly redefine the BC model, as in [18], such that the three configurations where *all* spins are on the same state become the zero temperature degenerate ground states. This redefinition ($x \to xc = \tilde{x}$) makes $\tilde{x}$ temperature independent; however, the results derived so far for the zeros on the complex $u = \mathrm{e}^h$ plane are still the same.

After this partial understanding of the conditions under which the Yang–Lee zeros remain on the unit circle, one might ask what we can say about the parameter region for which the Lee–Yang circle theorem is not valid. We do not have a nonperturbative approach to this question but we have made low temperature expansions (LTE) analogous to (30). First of all, we found useful to implement the redefinition $x \to xc = \tilde{x}$ before taking $c \to 0$. We emphasize that such a redefinition does not change the position of the zeros. Solving (26) by

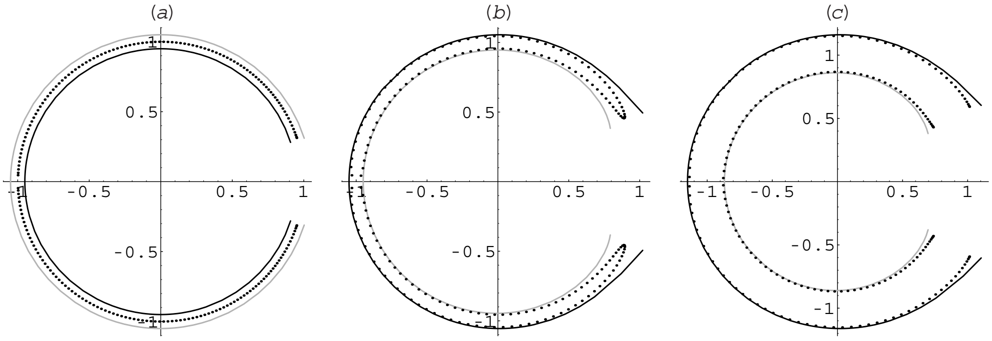

Figure 3. Overlap plot of ρ_+ (dark solid), ρ_- (light solid) and Yang–Lee zeros (dots) of the usual 1D Blume–Capel model at $c = 0.1$ and $\tilde{x} = 1.0$ (*a*), 1.1 (*b*) and 1.2 (*c*). In (*a*) the zeros lie on the unit circle. In all figures we used $n = 100$ spins (200 zeros).

a power series on c we have

$$\lambda_0 = \tilde{x} + \frac{2(A\tilde{x} - 1)\tilde{x}}{(\tilde{x} - \mathrm{e}^{h})(\tilde{x} - \mathrm{e}^{-h})}c + \mathcal{O}(c^2) \tag{31}$$

$$\lambda_\pm = \mathrm{e}^{\pm h}\left(1 + \frac{\tilde{x}}{\mathrm{e}^{\pm h} - \tilde{x}}c\right) + \mathcal{O}(c^2). \tag{32}$$

Defining $\mathrm{e}^h = \rho\,\mathrm{e}^{\mathrm{i}\alpha}$, imposing that $\Re e(f_+ - f_0) = 0$ or $\Re e(f_- - f_0) = 0$ we obtain respectively

$$\rho = \rho_+ = \tilde{x} + \frac{\tilde{x}(\tilde{x}^2\cos\alpha - 1)}{1 + \tilde{x}^4 - 2\tilde{x}^2\cos\alpha}c + \mathcal{O}(c^2)$$

$$\rho = \rho_- = \frac{1}{\tilde{x}} - \frac{(\tilde{x}^2\cos\alpha - 1)}{\tilde{x}(1 + \tilde{x}^4 - 2\tilde{x}^2\cos\alpha)}c + \mathcal{O}(c^2).$$

Note that, due to the $H \to -H$ symmetry which exchanges f_+ and f_- we have $\rho_+ = 1/\rho_-$. Assuming $|\lambda_+| = |\lambda_0|$ we are led to $\rho = \rho_+$, in this case we have calculated the difference

$$\Re e(f_+ - f_-) = 2\ln\tilde{x} + \frac{3(\tilde{x}^2\cos\alpha - 1)}{\tilde{x}^4 + 1 - 2\tilde{x}^2\cos\alpha}c + \mathcal{O}(c^2) \equiv F(\tilde{x}, c, \alpha). \tag{33}$$

Whenever $F > 0$ we have $|\lambda_+| = |\lambda_0| > |\lambda_-|$. If we had assumed $\rho = \rho_-$ in calculating $\Re e(f_+ - f_-)$ we would simply exchange the sign of the result, i.e., $\Re e(f_+ - f_-) = -F$ and consequently for $F > 0$ we would have $|\lambda_-| = |\lambda_0| > |\lambda_+|$. Concluding, for $F > 0$ the zeros may come either from $|\lambda_+| = |\lambda_0| > |\lambda_-|$ with $\rho = \rho_+$ or $|\lambda_-| = |\lambda_0| > |\lambda_+|$ with $\rho = \rho_-$ while for $F < 0$ they come from $|\lambda_+| = |\lambda_-| > |\lambda_0|$ with $\rho = 1$. Therefore, the form of the function F shows, at least for low temperatures, why the zeros departure from the unit circle as $\tilde{x}$ increases beyond $\tilde{x} = 1$. In figure 3 we plot ρ_+ and ρ_- for $c = 0.1$ and $\tilde{x} = 1, 1.1, 1.2$ altogether with the numerical results for the zeros for $n = 100$ spins.

We see that the zeros inside (outside) the unit circle basically come form $|\lambda_-| = |\lambda_0|(|\lambda_+| = |\lambda_0|)$ while the zeros on the unit circle originate from $|\lambda_+| = |\lambda_-|$. One can check that $F > 0$ for the cases of figures 3(*b*) and (*c*) but this is not true for figure 3(*a*) which explains the disagreement with the analytic curves. The large deviations which appear in the region close to the edges of the curves of zeros are consequences of the bad behaviour of the LTE around the Yang–Lee edge singularity. The same problem occurs in the LTE of the simpler case of the $s = 1/2$ 1D Ising model. In passing, we note that the Yang–Lee edge singularities can be obtained by imposing the degeneracy of the two largest eigenvalues of the transfer matrix as in [22]. We have used those singularities as a double check on the position of the zeros at the edges of the arcs. For the number of spins used in figure 3 the Yang–Lee singularities basically overlap with such zeros. In particular, in figure 3(c) there are four Yang–Lee edge singularities coinciding with the four edges of the two arcs. Finally, the reader may ask whether a triple degeneracy is possible, i.e., $|\lambda_+| = |\lambda_-| = |\lambda_0|$. In practice we never found this type of zero in our numerical results. After an exact analysis of the secular equation (26) we have found a necessary but not sufficient condition: $\tilde{x} > \sqrt{1+c}$.

3.2. 1D BC model on Feynman diagrams

We begin with the simplest case of the 1D Ising model on Feynman diagrams ($x = 0$). Only in this special case we have $\lambda_0 = 0$ and the polynomial $p_3(g)$ becomes a second order polynomial such that the $\mathcal{Z}_n^{nc}$, as given in (15), turn out to be proportional to Legendre polynomials ($\mathcal{P}_n$) as follows:

$$\begin{aligned}
\mathcal{Z}_n^{nc} &= \left[\frac{1}{\sqrt{\tilde{g}^2 - 2\tilde{g}\frac{\cosh(h)}{\sqrt{1-c^4}} + 1}}\right]_{g^n} \\
&= \left[\sum_{n=0}^{\infty} \tilde{g}^n \mathcal{P}_n\left(\frac{\cosh(h)}{\sqrt{1-c^4}}\right)\right]_{g^n} \\
&= \left[\frac{1+c^2}{(1-c^2)(1-c)^2}\right]^{n/2} \mathcal{P}_n\left(\frac{\cosh(h)}{\sqrt{1-c^4}}\right),
\end{aligned} \tag{34}$$

where $\tilde{g} = g\sqrt{1+c^2}/[(1-c^2)(1-c)^2]^{1/2}$.

It is known that polynomials which are orthogonal in the interval $[a, b]$ must have their zeros inside such an interval excluding the borders. Therefore, the zeros of the Legendre polynomials $\mathcal{P}_n(y_i) = 0; i = 1, \ldots, n$ are such that $-1 < y_i < 1$. The Yang–Lee zeros of the 1D Ising model on Feynman diagrams can thus be obtained from the zeros of the Legendre polynomials: $\cosh(h_j) = \sqrt{1-c^4}\, y_j$ which implies that the magnetic field is pure imaginary ($h_j = i\alpha_j$). So the Yang–Lee zeros must be on the unit circle on the complex $u = \mathrm{e}^h$ plane. This is so far the only exact proof of a circle theorem for statistical models defined on Feynman diagrams valid for finite number of spins. For two dimensions we found an analytic proof for the Ising model on Feynman diagrams with cubic vertices in [11] but valid only in the thermodynamic limit and inside the convergence region of the low temperature expansion.

In order to single out the effect of the Feynman diagrams on the zeros, it is interesting to compare the zeros that we have just found with the ones of the usual 1D Ising model with periodic boundary conditions (connected ring). We first note that each zero of the Legendre polynomial furnishes two Yang–Lee zeros $\pm\alpha_j^{nc}$ given by

$$\cos\alpha_j^{nc} = \sqrt{1-c^4}\, y_j. \tag{35}$$

For the usual 1D Ising model ($x = 0$) we have $\lambda_0 = 0$, see (26), and $\mathcal{Z}_n = \left(\lambda_+^n + \lambda_-^n\right)/c^n$. The Yang–Lee zeros come from $\lambda_\pm = r\,\mathrm{e}^{\pm\mathrm{i}\theta_k}$ where $\theta_k = (2k-1)\pi/(2n)$ with $k = 1, 2, \ldots, n$. From (26) we have $\lambda_+ + \lambda_- = A = 2\cosh(h)$ and $\lambda_+\lambda_- = (1-c^4)$. Therefore $r = \sqrt{1-c^4}$ and the zeros must be on the unit circle $h_j = \mathrm{i}\alpha_j$ with $\pm\alpha_j$ given by

$$\cos\alpha_j = \sqrt{1-c^4}\,\cos\frac{(2j-1)\pi}{2n}. \tag{36}$$

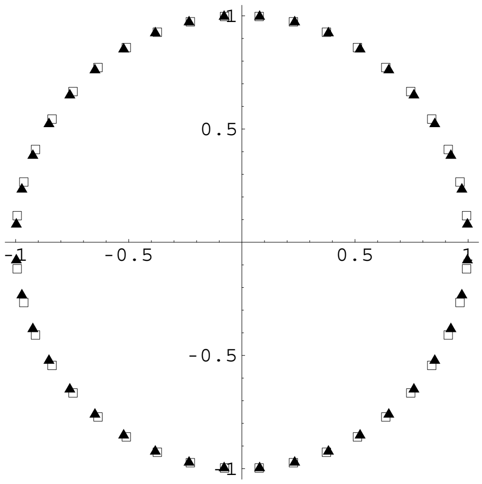

Figure 4. Yang–Lee zeros for the Ising model on a connected ring (empty squares) and on Feynman diagrams (filled triangles) at $c = 0.1$ and $n = 20$ spins.

Comparing (35) with (36) we see that, while the zeros of the model on the static lattice could be analytically determined, the sum over Feynman diagrams has led us to more complicated zeros, though still on the unit circle. Only numerical results can be obtained in general for zeros of Legendre polynomials. In the thermodynamic limit $n \to \infty$ we have asymptotic formulae for the zeros of Legendre polynomials, see, e.g., [24], at leading order: $y_k = \cos[(4k - 1)\pi/(4n + 2)]$ with $k = 1, 2, \ldots, n$. Using this formula it is easy to check that $\alpha_j - \alpha_j^{nc}$ is positive (negative) for zeros close to the positive (negative) real axis and it approaches zero at α close to $\pi/2$ in agreement with figure 4.

Besides, the difference $\alpha_j - \alpha_j^{nc}$ is of order $1/n^2$ in general which means that in the thermodynamic limit the zeros of the 1D Ising model on Feynman diagrams approach those of the model on the static lattice (one ring). At $n = 70$ spins we found already no visible difference between the zeros. This seems to be a general feature of the 1D spin models defined on Feynman diagrams as we will see later. It is remarkable that the zeros of the usual 1D Ising model with periodic boundary conditions are directly related, in the thermodynamic limit, with the zeros of Legendre polynomials.

Next we analyse the general case of the 1D BC model on Feynman diagrams for arbitrary x. Unfortunately, we have not been able to rewrite $\mathcal{Z}_n^{nc}$ in terms of orthogonal polynomials for $x \neq 0$. Thus, for finite number of spins we had to find the Yang–Lee zeros numerically. It turned out quicker to calculate the Gaussian integrals in expression (16) than to use formula (15). We found the zeros with great accuracy for diagrams with up to $n = 120$ spins, i.e., up to 240 zeros. We have checked for different temperatures, different values of $x = \mathrm{e}^{\Delta}$ and various number of spins that whenever the circle theorem holds for the usual 1D BC model it will also hold for the corresponding model on Feynman diagrams. So, there must be a generalization of the circle theorem for Feynman diagrams which is valid for finite size diagrams.

Furthermore, as we approach the thermodynamic limit we found in all cases that the Yang–Lee zeros on Feynman diagrams always tend to the zeros on the static lattice (one ring), see figure 5 where the zeros of the two models are already close for $n = 40$ spins. This

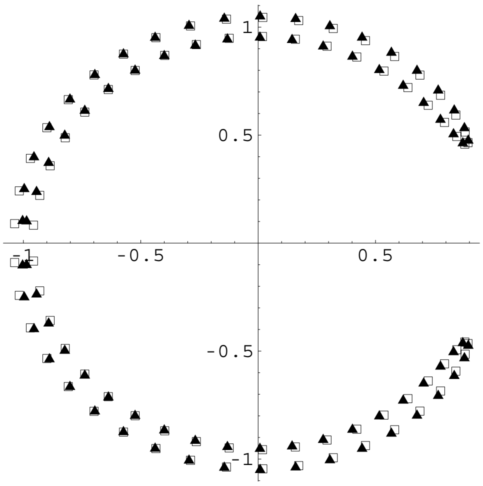

Figure 5. Yang–Lee zeros for the Blume–Capel model on a connected ring (empty squares) and on Feynman diagrams (filled triangles) at $c = 0.1$, $\tilde{x} = 1.1$ and $n = 40$ spins.

has been confirmed by an argument based on the saddle point equations as follows. After a redefiniton $\phi_a \to \sqrt{n}\phi_a$ in the numerator of (16) and calculating the denominator we obtain

$$\mathcal{Z}_n^{nc} = \frac{n^{n+3/2}(1-c^2)\sqrt{1-c}}{2^n n!(\pi/2)^{3/2}\sqrt{c}} \int \mathrm{d}\phi_+ \, \mathrm{d}\phi_- \, \mathrm{d}\phi_0 \, \mathrm{e}^{-nS} \tag{37}$$

where $S = S_{g=0} - \ln V$ with $V = \mathrm{e}^h \phi_+^2 + \mathrm{e}^{-h}\phi_-^2 + \mathrm{e}^{\Delta}\phi_0^2$. The saddle point equations defined by $\partial_a S = 0$ are given by

$$\begin{aligned} \phi_+ - (1+c)\,\phi_0 + c\phi_- &= \frac{2\,\mathrm{e}^h \phi_+}{V} \\ \phi_- - (1+c)\,\phi_0 + c\phi_+ &= \frac{2\,\mathrm{e}^{-h} \phi_-}{V} \\ f\phi_0 - (1+c)\,(\phi_+ + \phi_-) &= \frac{2\,\mathrm{e}^{\Delta}\phi_0}{V}. \end{aligned} \tag{38}$$

It is easy to combine the above equations to show that at all saddle points (s.p.) solutions we have $S_{g=0} = 1$ and V satisfies a cubic equation such that $(1-c^2)(1-c)V/2 \equiv \lambda$ satisfies precisely (26). Thus, the six solutions of the saddle point equations are doubly degenerated since they produce only three different values for S at leading order. Expanding about the saddle points $\phi_a = \tilde{\phi}_a + \zeta_a/\sqrt{n}$ we have up to quadratic terms $S = \tilde{S} + (\zeta_a\zeta_b\partial_a\partial_b S|_{\text{s.p.}})/2n$. Integrating over the fluctuations $\mathrm{d}\zeta_a$ and using Stirling's approximation we have at leading order

$$\mathcal{Z}_n^{nc} = \frac{2(1-c^2)\sqrt{1-c}}{\sqrt{2\pi nc}} \left[\frac{1}{(1-c^2)(1-c)}\right]^n \sum_{\text{s.p.}} \frac{\lambda_{\text{s.p.}}^n}{\sqrt{\det \partial_a\partial_b S|_{\text{s.p.}}}} \tag{39}$$

where the factor 2 in the numerator comes from the double degeneracy of the saddle point solutions and $\lambda_{\text{s.p.}}$ can only be λ_+, λ_- or λ_0. If we compare the symmetry factors in (21) we note that the more non-connected diagrams like the first one between brackets drop out at $n \to \infty$. However, at this limit, see (21), the connected diagram is not the only one to survive. If we remember the solution of the usual connected partition function (25) and look at (39) we realize that the effect of the other partition functions of the same order as $\mathcal{Z}_n$ is to produce the denominators $\sqrt{\det \partial_a\partial_b S|_{\text{s.p.}}}$.

The sum in (39) extends over all relevant saddle points. In order to single out which solutions of (38) are relevant, a careful analysis of the absolute values of λ_a would be necessary which depends in general on the parameters $c, \mathrm{e}^{\Delta}, \mathrm{e}^{h}$ and is rather complicated if we want an exact result. Instead, we discuss the case of the Ising model ($x = 0$) and assume that the general case will be similar as our numerical results for finite number of spins seem to indicate. For the Ising model we know that $\mathcal{Z}_n^{nc}$ are proportional to Legendre polynomials for which asymptotic formulae are known, see, e.g., [24] so we can check the result. If $x = 0$ we have $\lambda_0 = 0$. We are thus left with two doubly degenerated saddle point solutions. We assume that they all contribute whenever $|\lambda_+| = |\lambda_-|$ which means $\lambda_\pm = \sqrt{1-c^4}\,\mathrm{e}^{\pm\mathrm{i}\theta}$. In this case (39) becomes,

$$\mathcal{Z}_n^{nc} = \frac{2\sqrt{1-c^4}}{\sqrt{4\pi n}(1-c^2)^n(1-c)^n}\left\{\frac{\lambda_+^n}{[\lambda_-(\lambda_+-\lambda_-)]^{1/2}} + \frac{\lambda_-^n}{[\lambda_+(\lambda_--\lambda_+)]^{1/2}}\right\} \tag{40}$$

$$= \left[\frac{1+c^2}{(1-c^2)(1-c)^2}\right]^{n/2}\sqrt{\frac{2}{\pi n}}\frac{\sin\left[\left(n+\frac{1}{2}\right)\theta+\frac{\pi}{4}\right]}{(2\sin\theta)^{1/2}}. \tag{41}$$

The above expression reproduces exactly, including the overall constant asymptotic formulae for Legendre polynomials at leading order [24], compared with (34), which shows *a posteriori* that all four saddle point solutions (doubly degenerated) must contribute. The Yang–Lee zeros correspond to $\cos\alpha = \sqrt{1-c^4}\cos[(4k-1)\pi/(4n-2)]$ with $k = 0,\ldots,n$ as we mentioned before. Since $\lambda_\pm$ are the solutions of equation (26) with $\tilde{x} = 0$, i.e., $\lambda_\pm = \cosh(h) \pm \sqrt{\cosh^2 + c^4 - 1}$. If h and c are real both $\lambda_\pm$ are also real and $\lambda_+ > \lambda_-$. In this case $\det\partial_a\partial_b S < 0$ at the second solution, see second term in (40). Thus, the steepest descent trajectory only passes by the first saddle point, the second point is not a true saddle point. Once again we reproduce asymptotic formulae for $\mathcal{P}_n(y)$ for $y > 1$. In particular, the free energy of the model on Feynman diagrams is the same one of the traditional 1D Ising model on a ring up to the addition of a constant.

As a final comment concerning the 1D model Ising on Feynman diagrams, we mention that the condition $\det\partial_a\partial_b S = 0$ at the saddle points gives rise presumably [15] to continuous phase transitions. In our case this implies that the Yang–Lee edge singularity of the Ising model defined on Feynman diagrams coincides with the same singularity in the usual 1D Ising model, i.e., $\lambda_+ = \lambda_-$.

For the general case of the 1D BC model on Feynman diagrams, once again the zeros can only appear whenever the absolute value of, at least, two eigenvalues λ_a degenerate, which is the same basic equation for the zeros that we have obtained when discussing the traditional 1D BC model on a ring. This equation gives $\rho = \rho(\alpha)$ in the complex $\mathrm{e}^h = \rho\,\mathrm{e}^{\mathrm{i}\alpha}$ plane. The precise values for α will be fixed by the relative phases of the saddle points which are present in the factors $\sqrt{\det\partial_a\partial_b S|_{\text{s.p.}}}$. According to our numerical results for finite number of spins we believe that the α_k will be close to their corresponding counterparts in the connected (traditional) 1D BC model.

3.3. Conclusion

Concerning the usual 1D Blume–Capel model defined on a connected ring (periodic boundary conditions) our numerical results have shown that their Yang–Lee zeros remain on the unit circle as far as either $\Delta \leqslant \ln 2$ or $\Delta \leqslant K$. The first condition has been known for many years [4] to be sufficient, in arbitrary dimensions, to rewrite the Blume–Capel model in such a way that the original Lee–Yang circle theorem applies. The second one is new and it is not clear whether it only works in the one-dimensional case. We have presented a perturbative proof of this second condition valid for small $e^{\Delta-K}$. Furthermore, we have observed that as a general feature as we increase Δ or the temperature or even both of them, the zeros which lie originally on the unit circle tend to bifurcate as in the two-dimensional case [18], although no phase transition is present for real magnetic fields and non-vanishing temperature in one dimension. At some point (Δ^*, K^*) two disjoint arcs appear. We have shown by a low temperature expansion that the existence of two curves can be understood from the degeneracy of the absolute value of the transfer matrix eigenvalues. One of the curves comes from $|\lambda_+| = |\lambda_0|$ while the other one is due to $|\lambda_-| = |\lambda_0|$. For the zeros which remain on the unit circle the degeneracy condition is $|\lambda_+| = |\lambda_-|$.

Regarding the 1D Blume–Capel model defined on Feynman diagrams, which includes a sum over connected and non-connected rings, although its partition function is rather complicated, see (21), its zeros seem to follow, especially for large rings, the same pattern of the corresponding model defined on a connected ring. In particular, the two previously mentioned conditions are apparently satisfied. We have not been able to furnish a rigorous proof of this fact in general but an argument based on the saddle point solutions show that the conditions for Yang–Lee zeros are the same degeneracy conditions of the last paragraph. We believe that this is a general feature of models defined on the type of dynamical lattice used here. This indicates that a generalization of the circle theorem for dynamical lattices might exist. In fact, in the special case of the 1D Ising model $\Delta \to -\infty$ we have proved that the Yang–Lee zeros of the model defined on Feynman diagrams do lie on the unit circle. This is the only rigorous proof we know valid for dynamical lattices and finite number of degrees of freedom. It is not clear whether the polynomials can be written in the form used in the original proof of the circle theorem in [2] or whether this proof is an independent one. Remarkably, it turns out that the zeros in the variable e^h of the partition function of the usual 1D Ising model with periodic boundary conditions are directly related in the thermodynamic limit with the zeros of the Legendre polynomials.

Finally, we remark that throughout this paper we have obtained the partition function of usual 1D models with periodic boundary conditions (one ring) by taking the logarithm of the generating function of all diagrams including non-connected ones. This well-known result in diagrammatic expansions furnishes an alternative to the usual abstract but simpler transfer matrix approach in solving exactly 1D models. It has already proven to be useful from the computational point of view since it became quicker than using solutions of the secular equation and plugging back in the partition function.

Acknowledgments

This work was supported by CNPq, CAPES-Proap and FINEP (cc@complex). DD acknowledges a discussion on connected diagrams with Luis C de Albuquerque and an e-mail exchange with Nelson A Alves.

References

[1] Yang C N and Lee T D 1952 *Phys. Rev.* **87** 404
[2] Lee T D and Yang C N 1952 *Phys. Rev.* **87** 410
[3] Griffiths R B 1969 *J. Math. Phys.* **10** 1559
[4] Suzuki M 1973 *J. Math. Phys.* **14** 1088
[5] Suzuki M and Fisher M E 1971 *J. Math. Phys.* **12** 235

[6] Asano T 1970 *Phys. Rev. Lett.* **24** 1409
[7] Dunlop F and Newman C M 1975 *Commun. Math. Phys.* **44** 223
[8] Staudacher M 1990 *Nucl. Phys.* B **336** 349
[9] Ambjorn J, Anagnostopoulos K N and Magnea U 1998 *Nucl. Phys.* B **63** 751
Ambjorn J, Anagnostopoulos K N and Magnea U 1997 *Mod. Phys. Lett.* A **12** 1605
[10] Janke W, Johnston D A and Stathakopoulos M 2001 *Nucl. Phys.* B **614** 494
[11] de Albuquerque L C, Alves N A and Dalmazi D 2000 *Nucl. Phys.* B **580** 739
[12] Kazakov V A 1986 *Phys. Lett.* A **119** 140
Boulatov D and Kazakov V A 1987 *Phys. Lett.* B **186** 379
[13] Bachas C, de Calan C and Petropoulos P 1994 *J. Phys. A: Math. Gen.* **27** 6121
[14] Dolan B P, Janke W, Johnston D A and Stathakopoulos M 2001 *J. Phys. A: Math. Gen.* **34** 6211
[15] Johnston D A 1998 *J. Phys. A: Math. Gen.* **31** 5641
[16] de Albuquerque L C and Dalmazi D 2003 *Phys. Rev.* E **67** 66108
[17] Blume M 1966 *Phys. Rev.* **141** 517
Capel H W 1966 *Physica* **32** 966
[18] Biskup M, Borgs C, Chayes J T, Kleinwaks L J and Kotecky R 2000 *Phys. Rev. Lett.* **84** 4794
[19] Blume M, Emery V J and Griffiths R B 1971 *Phys. Rev.* A **4** 1071
[20] Bessis D, Itzykson C and Zuber J B 1980 *Adv. Appl. Math.* **1** 109
[21] Glumac Z and Uzelac K 1994 *J. Phys. A: Math. Gen.* **27** 7709
[22] Wang Xian-Zhi and Kim J S 1998 *Phys. Rev* E **58** 4174
[23] Ising E 1925 *Z. Phys.* **31** 253
[24] Bender C M and Orszag S A 1999 *Advanced Mathematical Methods for Scientistis and Engineers* (Berlin: Springer)